A Study on Radiation Damage in BGO and PWO-II Crystals

2012 J. Phys.: Conf. Ser. 404 012025

(http://iopscience.iop.org/1742-6596/404/1/012025)

Journal of Physics: Conference Series **404** (2012) 012025 doi:10.1088/1742-6596/404/1/012025

A Study on Radiation Damage in BGO and PWO-II Crystals

Fan Yang, Rihua Mao, Liyuan Zhang and Ren-Yuan Zhu
256-48, HEP, California Institute of Technology, Pasadena, CA 91125, USA
E-mail: zhu@hep.caltech.edu

Abstract. We report in this paper an investigation on radiation damage in 20 cm long BGO crystals produced at SIC as well as 20 cm long PWO-II crystals produced at BTCP for the proposed Panda experiment at GSI. The optical and scintillation properties of BGO and PWO-II crystals, such as transmittance, light output and light response uniformity, were measured before and after γ-ray irradiations at different dose rates. BGO crystals produced recently are compared to crystals used in the L3 experiment at LEP which was produced in early eighties. PWO-II crystals are compared to crystals used in the CMS experiment. Progresses are observed in the radiation hardness for both crystals. Their use for crystal calorimeters in future high energy physics experiments is discussed. To maintain crystal precision, a precision light monitoring system is mandatory to trace variations of crystal transparency *in situ* for a BGO or PWO crystal calorimeter in radiation environment.

1. Introduction

Because of their high density (7.13 g/cm^3 and 8.3 g/cm^3), short radiation length (1.12 cm and 0.89 cm), $Bi_4Ge_3O_{12}$ (BGO) and $PbWO_4$ (PWO) crystals have been used to construct electromagnetic calorimeters (ECAL) for high energy physics (HEP) experiments, such as the L3 experiment at LEP [1] and the CMS experiment at LHC [2]. They are also being considered for future HEP experiments, where precision measurements of photons and electrons are crucial for their physics mission. The use of large size scintillation crystals in future HEP experiment, however, faces a challenge from the severe radiation environment expected in these experiments. Recently, BGO and PWO crystals with improved radiation hardness were grown at Shanghai Institute of Ceramics (SIC) and Bogoroditsk Techno-Chemical Plant (BTCP). In this paper, we present a study of the radiation hardness for large size BGO and PWO-II crystals grown recently, and compare them to the crystals used for the L3 and CMS experiment respectively.

Figure 1. BGO samples used in this study

Figure 2. PWO samples used in this study

Fig.1 shows the BGO samples investigated in this study. The two rectangular samples were grown in 2004 and 2011 at SIC, and have a dimension of 25×25×200 mm^3. The tapered BGO sample was grown at SIC in 1980 for the L3 experiment with a dimension of 20×20 mm^2 at the small end, 30×30 mm^2 at the large end and 240 mm in length. Fig.2 shows PWO samples investigated. Two shorter samples are PWO-II crystals grown recently at BTCP for the proposed Panda experiment [3] with a dimension of 24.5×24.5×200 mm^3. Two longer samples are typical PWO crystals grown at SIC and BTCP for the CMS experiment. A total of 52 CMS PWO samples were studied in our previous study [4], in which 21 from BTCP and 32 from SIC. All 21 BTCP samples are of the CMS endcap size with a slightly tapered shape: 28.5×28.5 mm^2 at the small end, 30×30 mm^2 at the large end and 220 mm long. Among the 32 samples from SIC, 20 samples have a rectangular shape of 22×22×230 mm^3 and the other 12 are of the CMS endcap size. All six faces of these BGO and PWO samples are polished.

Longitudinal transmittance (LT) was measured using a PerkinElmer LAMBDA 950 UV/Vis spectrophotometer with double beam, double monochromator and a large sample compartment equipped with an integrating sphere. The systematic uncertainty in repeated measurements was about 0.15%. Scintillation light output (LO) was measured before and after irradiations by using a Hamamatsu R1306 PMT with a bi-alkali photo-cathode and a borosilicate glass window for BGO, and a Hamamatsu R2059 PMT with a bi-alkali photo-cathode and a quartz window for PWO. For the LO measurement, the large (tapered samples) or one (rectangular samples) end of the samples was coupled to the corresponding PMT with Dow Corning 200 fluid, while all other faces of the sample were wrapped with Tyvek paper. A collimated ^{137}Cs source was used to excite the samples. The γ-ray peak positions were obtained by a simple Gaussian fit.

The γ-ray irradiations were carried out in two facilities at Caltech: a 50 curie ^{60}Co source for irradiations at low dose rates (2, 8 and 30 rad/h) and a 7,000 curie ^{137}Cs source for high dose rate at 7,160 rad/h. The dose rates were calibrated. The main consequence of γ-ray induced radiation damage in BGO and PWO crystals is radiation induced absorption which causes degradation of transmittance and light output [5,6]. It may also affect crystal's light response uniformity (LRU) and cause a degradation of the energy resolution if the light attenuation length (LAL) is reduced significantly [7,8]. The γ-ray induced absorption may also spontaneously recover, leading to a dose rate dependent radiation damage [5].

2. Gamma ray induced radiation damage in BGO crystals

2.1 Initial properties

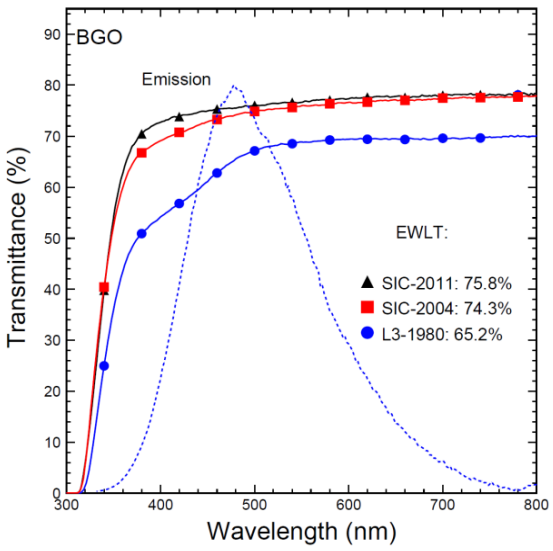

Figure 3. Initial LT and EWLT of BGO samples

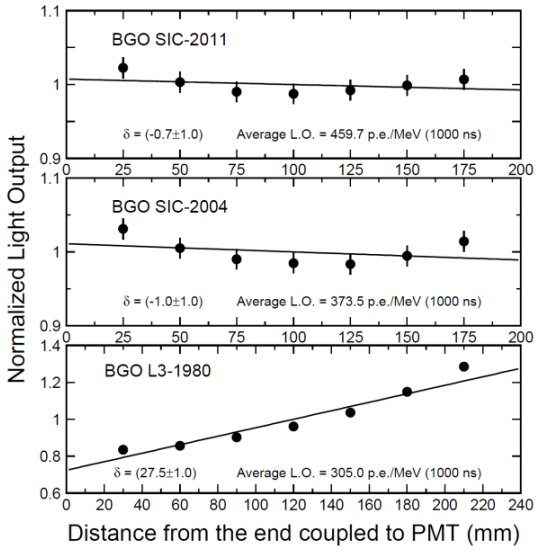

Figure 4. Initial LO and LRU of BGO samples

All three BGO crystals were annealed at 200℃ for 200 minutes and then irradiated by γ-ray at 2, 8, and 30 rad/h step by step until reaching equilibrium, following which recovery measurement was carried out.

Fig.3 shows longitudinal transmittance and the emission for all samples before irradiations. Also shown in the figure is the numerical value of the emission weighted longitudinal transmittance (EWLT), which is defined as:

$$EWLT = \frac{\int LT(\lambda)Em(\lambda)d\lambda}{\int Em(\lambda)d\lambda} \qquad (1)$$

The EWLT is a good representation of crystal's transparency better than the transmittance at the emission peak. Comparing with other BGO samples, sample SIC-2011 shows the best LT and the highest EWLT, indicating a clear progress in crystal's optical property.

Fig. 4 shows the LO and LRU before irradiations for all samples. The LRU was measured by moving a collimated γ-ray source along the longitudinal axis of the long sample at seven evenly distributed points. The response (y) was fit to a linear function:

$$\frac{y}{y_{mid}} = 1 + \delta(\frac{x}{x_{mid}} - 1) \qquad (2)$$

where y_{mid} represents the light output at the middle of the crystal, δ represents the shape of the LRU; x is the distance from one end of the crystal. It is clear that sample SIC-2011 has the best LO among three samples. While both rectangular crystals have a flat response, the response of the L3 BGO at the far (small) end is significantly higher than that at the near (large) end which is coupled to the PMT. This is due to a well-known optical focusing effect caused by the tapered geometry of this sample.

2.2 γ-ray induced radiation damage and its recovery

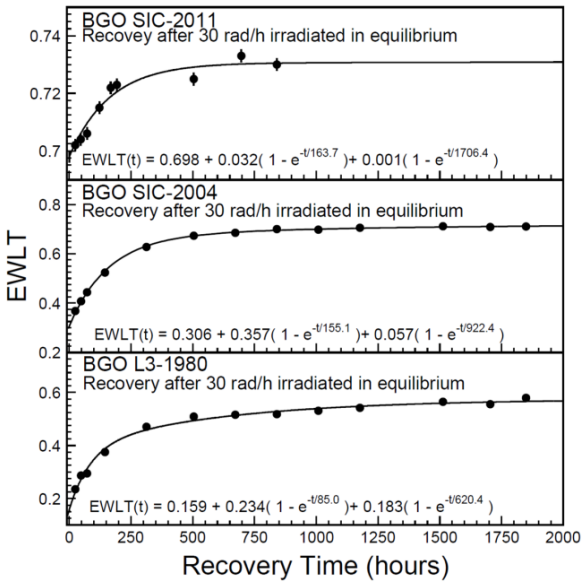

Figure 5. Recovery of EWLT for all samples after reaching equilibrium at 30 rad/h

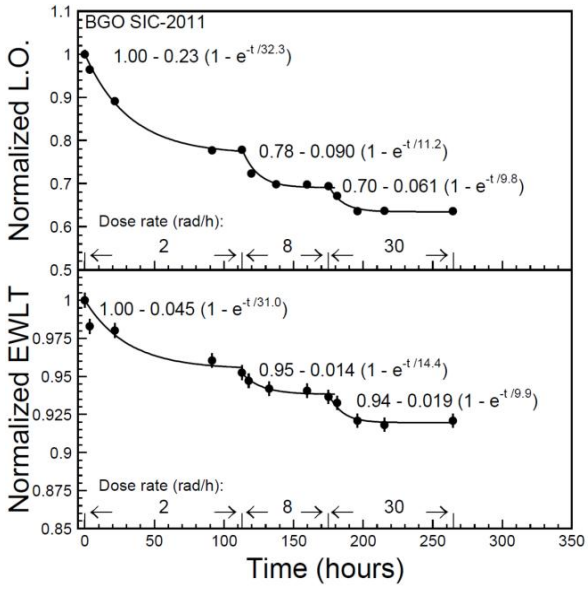

Figure 6. Normalized LO and EWLT for sample SIC-2011 under γ-ray irradiations

Fig. 5 shows the γ-ray induced radiation damage (EWLT) recovers under room temperature. All three crystals were irradiated at 2, 8, and 30 rad/h step by step until reaching equilibrium, following which recovery was measured. Two time constants were determined by an exponential fit to describe the recovery process, indicating at least two color centers at different depth. Comparing to the initial

EWLT (75.8%, 74.3% and 65.2% respectively for sample SIC-2011, SIC-2004 and L3-1980), the EWLT values measured after a few thousands hours recovery is significant lower, indicating additional deep color centers in these crystals.

Because of the recovery, the γ-ray induced radiation damage in BGO is dose rate dependent. The degradation of both LT and LO under a certain dose rate would reach an equilibrium, when the speed of the color center formation (damage) equals to the speed of the color center annihilation (recovery) [5]. Fig. 5 shows the normalized LO and EWLT for sample SIC-2011 during γ-ray irradiations in three steps at dose rates of 2, 8 and 30 rad/h. Both EWLT and LO reached equilibrium during irradiations under a defined dose rate, showing a clear dose rate dependent damage. Consistent time constants were determined by exponential fits for both normalized LO and EWLT.

2.3 Radiation damage as a function of the dose rate

Fig. 7 shows the normalized LO and EWLT measured in equilibrium as a function of the dose rate for all three samples. The corresponding data are listed in Table 1. It is clear that progress has been made in the radiation hardness of sample SIC-2011 as compared to other two BGO crystals produced early.

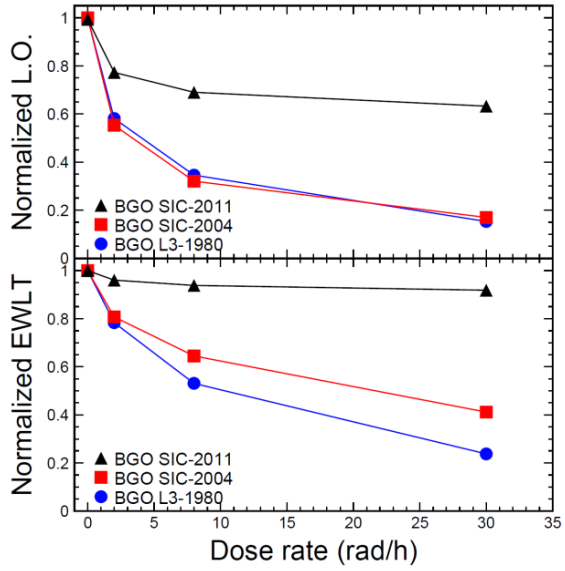

Figure 7. Normalized LO and EWLT as a function of the dose rate

Table 1. LO and EWLT loss of BGO samples in equilibrium under different dose rates

Samples		SIC-2011	SIC-2004	L3-1980
Initial LO (p.e./MeV)		460	373	305
Initial EWLT (%)		75.8	74.3	65.2
LO Loss (%)	2rad/h	22	45	42
	8rad/h	31	68	66
	30rad/h	36	83	85
EWLT Loss (%)	2 rad/h	4	19	22
	8 rad/h	6	36	47
	30rad/h	8	59	76

3. Gamma ray induced radiation damage in PWO-II crystals

Two PWO-II crystals were annealed at 200℃ for 200 minutes to remove residual radiation damage and then irradiated at 2, 8, 30 and 7,160 rad/h step by step until reaching equilibrium in each step. It is well known that the γ-ray induced radiation damage in PWO crystals recovers under room temperature, leading to dose rate dependent radiation damage [6,7]. Their recovery was measured after 30 rad/h in equilibrium. The radiation damage data of these two PWO-II samples are compared to that of CMS PWO crystals [4].

3.1 Initial properties and recovery of radiation induced damage

Fig. 8 shows correlations between the numerical values of the initial LO and the initial LT at 360 nm for PWO crystals grown at SIC (top) and BTCP (bottom). Also shown in these figures are the linear fits to the data and the linear correlation coefficients (CC), defined as:

$$CC = \frac{\sum(x-\bar{x})(y-\bar{y})}{\sqrt{\sum(x-\bar{x})^2 \sum(y-\bar{y})^2}} \qquad (3)$$

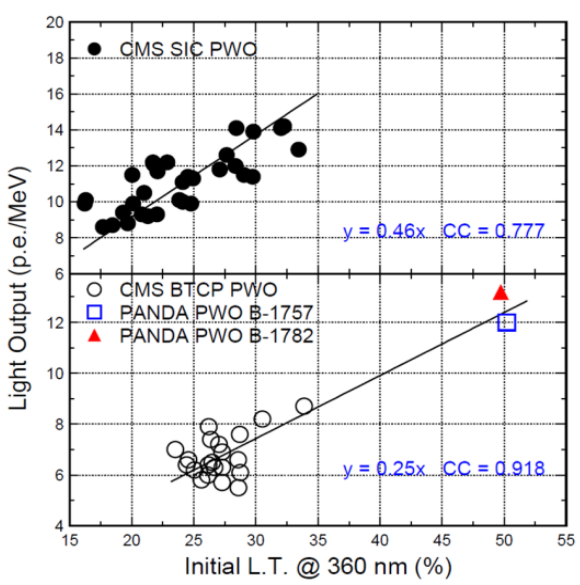

Figure 8. Correlations between the initial LO and the initial LT at 360 nm

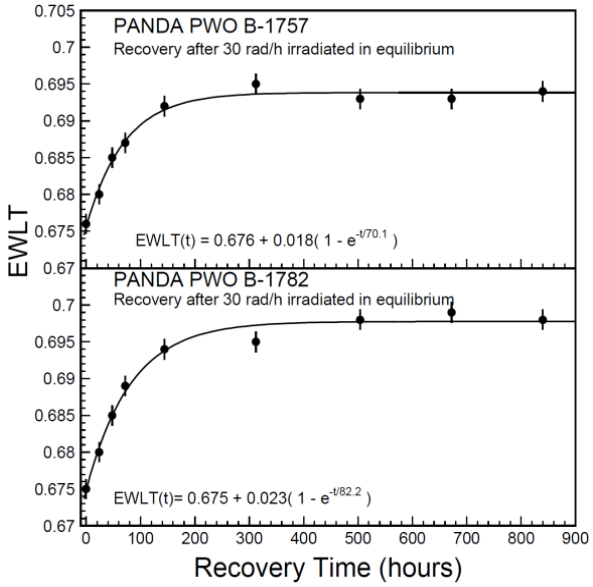

Figure 9. Recovery of EWLT as irradiated at 30 rad/h in equilibrium

The LT values of PWO-II crystals at 360 nm are significantly higher than CMS crystals. Their light output is also higher than the CMS PWO crystals grown at BTCP, but is compatible with the CMS PWO crystals grown at SIC. We note that the BTCP samples have a higher longitudinal transmittance values at 360 nm as compared to the SIC samples. This is partly due to the birefringent nature of the PWO crystals. While the BTCP PWO crystals were grown along the "a" axis the SIC crystals were grown along the "c" axis [4]. Because of the birefringence PWO crystals grown along the "a" axis should have higher theoretical limit of transmittance than that grown along the "c" axis. The linear fits also show different slopes for the SIC and BTCP samples, which may also be caused by their different crystal orientations. The nature of this correlation is understood due to the self-absorption effect: the very blue part of the PWO emission spectrum is self-absorbed because of the cross-over of the transmittance and emission spectra at 360 nm [4].

Both PWO-II crystals were irradiated at 2, 8, 30 and 7,160 rad/h step by step until reaching equilibrium. Fig. 9 shows the recovery of EWLT under room temperature for two PWO-II samples after 30 rad/h irradiations in equilibrium. Consistent recovery time constants were determined by exponential fits. The initial EWLT values (70.0% and 70.1% for sample B-1757 and B-1782), however, are not reached after nine hundreds hours' recovery, indicating deep color centers in these PWO crystals.

3.2 Radiation damage as a function of dose rate

Fig. 10 shows normalized LO (top) and EWLT (bottom) as a function of the dose rate for two PWO-II samples in equilibrium. The corresponding data are listed in the Table 2. The LO loss of PWO-II crystals is about 45% at 7,160 rad/h in equilibrium and corresponding EWLT loss is about 10%. These two PWO-II crystals have consistent radiation harness up to 7,160 rad/h.

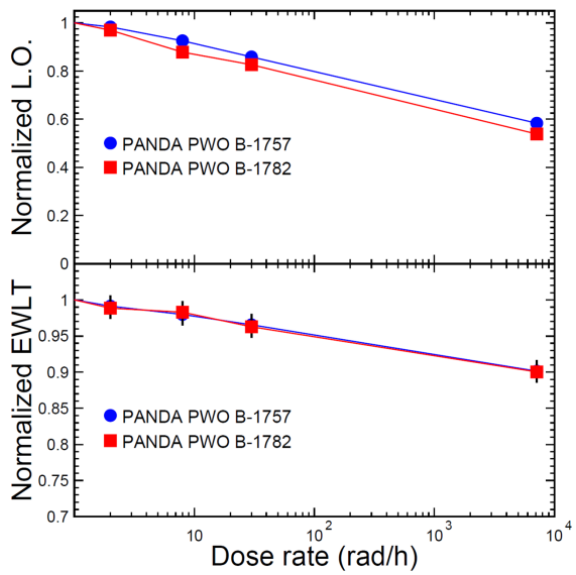

Figure 10. Normalized LO and EWLT as a function of the dose rate for PWO-II crystals

Table 2 LO and EWLT loss of PWO samples in equilibrium under different dose rates

Samples		PWO B-1757	PWO B-1782
Initial LO (p.e./MeV)		12.0	13.2
Initial EWLT (%)		70.0	70.1
LO Loss (%)	2rad/h	2	3
	8rad/h	8	12
	30rad/h	14	17
	7160rad/h	42	46
EWLT Loss (%)	2 rad/h	0.8	1.1
	8 rad/h	2.0	1.7
	30rad/h	3.4	3.7
	7160rad/h	9.9	10.0

3.3 Comparison of radiation hardness for PANDA PWO-II and CMS PWO

The radiation induced absorption coefficient and the emission weighted radiation induced absorption coefficient (EWRIAC) can be extracted from the LT data measured before and after irradiations [9,10]. The EWRIAC is a measure of the radiation damage, which is defined as

$$EWRIAC = \frac{\int RIAC(\lambda)Em(\lambda)d\lambda}{\int Em(\lambda)d\lambda}, \qquad (4)$$

where *RIAC* is the radiation induced absorption coefficient or the radiation induced color center density, and *Em* is the scintillation emission as a function of wavelength. The *RIAC* can be calculated as the difference of the color centers represented as the inverse of the light attenuation length (LAL):

$$RIAC = \frac{1}{LAL_{equilibrium}} - \frac{1}{LAL_{before}}, \qquad (5)$$

where "equilibrium" refers to "in equilibrium", and "before" refers to "before irradiation". The light attenuation length was calculated by using the longitudinal transmittance data according to:

$$\mathrm{LAL} = \frac{l}{\ln\left\{[\mathrm{T}(1-\mathrm{T}_S)^2]/\left[\sqrt{4T_S^4+T^2(1-\mathrm{T}_S)^2-2T_S^2}\right]\right\}}, \qquad (6)$$

where T is the transmittance measured along crystal length l and T_S is the theoretical transmittance without internal absorption.

Fig. 11 shows correlations between the relative LO losses versus the relative LT losses at 440 nm (top) and the corresponding EWRIAC values (bottom) for all PWO samples in the equilibrium. Positive correlations are observed with the linear correlation coefficient at 50% level. The data of PWO-II crystals groups well with the data of CMS PWO crystals. The good correlation between the LO losses versus the LT losses at 440 nm indicates that the LT at 440 nm is a good measure of the radiation damage. This result is consistent with our previous investigation where 440 nm was chosen for the monitoring wavelength because of its best linearity [11].

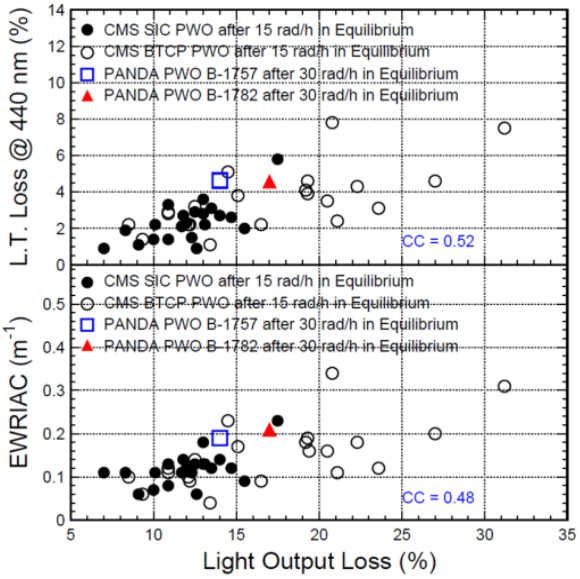

Figure 11. Correlations between the LO loss versus the LT loss at 440 nm (top plot) and the EWRIAC (bottom plot) for all PWO crystals

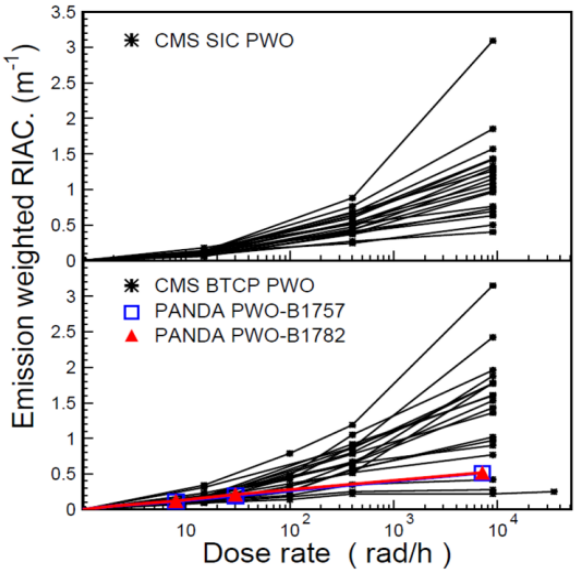

Figure 12. Distributions of the EWRIAC as a function of the dose rate

Fig. 12 shows distributions of the EWRIAC values as a function of the γ-ray dose rate. It is clear that two PWO-II crystals are in the better portion of the CMS PWO crystals. The EWRIAC values of PWO-II crystals are less than 0.5 m^{-1} up to 7,160 rad/h, indicating no damage to the light response uniformity for PWO-II crystals under such dose rate

4. Summary

Significant progress is observed in both BGO crystals grown at SIC and PWO crystals grown at BTCP. The BGO sample SIC-2011 has the better initial LT and LO as well as a better radiation hardness than previous BGO samples. It is radiation hard up to 30 rad/h. Investigation will continue for these BGO samples at high dose rate. PWO-II samples have a better LT at 360 nm and LO as compared to CMS PWO crystals. Their radiation hardness is in the better portion of the CMS PWO crystals. They are radiation hard up to 7,160 rad/h. Correlations are confirmed between: (1) LO and LT at 360 nm, (2) LO loss versus LT loss at 440 nm, and (3) LO loss versus EWRIAC.

Radiation damage in BGO and PWO crystals recovers under room temperature, leading to a dose rate dependent damage level. Because of the recovery, a precision light monitoring system is mandatory for a BGO or PWO crystal calorimeter in a radiation environment to trace variations of crystal transparency and provide crucial monitoring corrections for inter-calibration *in situ*.

Acknowledgments

The authors would like to thank Prof. Shaohua Wang of SIC and Prof. R. Novotny of the Giessen University for providing BGO and PWO-II samples respectively used in this study. This work was supported in part by the US Department of Energy Grant DE-FG03-92_ER40701.

References

[1] U. Micke 1987 *Helv Phys Acta* **60**, 685.

[2] E. Auffray 2001 *Nucl Instrum Meth A* **461**, 365.

[3] R. W. Novotny 2004 *IEEE T Nucl Sci* **51**, 3076.

[4] J. M. Chen, R. H. Mao, L. Y. Zhang, and R. Y. Zhu 2007 *IEEE T Nucl Sci* **54**, 375.

[5] R. Y. Zhu 1998 *Nucl Instrum Meth A* **413**, 297.

[6] R. Y. Zhu, H. Stone, H. Newman, T. Q. Zhou, H. R. Tan, and C. F. He 1991 *Nucl Instrum Meth A* **302**, 69.

[7] R. Y. Zhu 1997 *IEEE T Nucl Sci* **44**, 468.

[8] D. A. Ma and R. Y. Zhu 1993 *Nucl Instrum Meth A* **332**, 113.

[9] R. H. Mao, L. Y. Zhang, and R. Y. Zhu 2004 *IEEE T Nucl Sci* **51**, 1777.

[10] D. A. Ma and R. Y. Zhu 1993 *Nucl Instrum Meth A* **333**, 422.

[11] X. D. Qu, L. Y. Zhang, and R. Y. Zhu 2000 *IEEE T Nucl Sci* **47**, 1741.